Spin tunneling into Si measured by three-terminal Hanle signals in vertical and lateral Si devices with Fe/Mg/MgO/Si tunnel junctions

Shoichi Sato[1], Ryosho Nakane[1,2], Mitsuki Ichihara[1], Takato Hada[1], and Masaaki Tanaka[1,3]

[1] Department of Electrical Engineering and Information Systems, The University of Tokyo
[2] Institute for Innovation in International Engineering Education, The University of Tokyo
[3] Center for Spintronics Research Network (CSRN), The University of Tokyo
7-3-1, Hongo, Bunkyo-ku Tokyo 113-8654, Japan
Phone: +81-3-5841-6729   E-mail: satodaikon@cryst.t.u-tokyo.ac.jp

Abstract

We have investigated spin tunneling into Si by measuring three-terminal Hanle (3TH) signals in devices with Fe/Mg/MgO/Si junctions prepared on a bulk Si and a thin-body Si-on-insulator (SOI) substrates. In vertical three-terminal devices with the bulk Si substrate, the magnitude of the broader 3TH signal (the parasitic magnetoresistance of the tunnel junction) decreases and the narrower 3TH signal (the spin accumulation signal in the Si channel) appears, when a magnetically-dead layer was prevented by inserting a Mg layer between the Fe and MgO layers. This result agrees well with the "dead-layer model" reported in our previous paper. In a multi-terminal lateral device, the narrower 3TH signal was enhanced by the channel confinement effect with the thin Si channel, although the broader 3TH signal remains unchanged.   The result is also the evidence that the narrower Hanle signal is the spin accumulation signal, but the broader Hanle signal is not.

1. Introduction

Recently, many spin-dependent transport studies using ferromagnetic metal (FM)/oxide (Ox) /Si tunnel structures showed two types of three-terminal (3T) Hanle signals; narrower Hanle signal (N-3TH) and broader Hanle signal (B-3TH) [1,2]. The origin of N-3TH is the spin accumulation in the Si, whereas that of B-3TH is still under discussion [3]. Our theory and experiment showed that a magnetically-dead layer formed at a FM/Ox interface causes B-3TH and also reduces N-3TH due to the degradation of spin injection efficiency into Si [4]. In this study, we experimentally demonstrate that the spin injection efficiency is enhanced when the formation of magnetically-dead layer is prevented by inserting a Mg layer at the Fe/MgO interface [5]. To ensure our findings, we also investigate and compare the 3TH signals in vertical and lateral devices using the function that takes the device geometry into account.

2. Sample preparation and measurement setups

Figure 1(a) show our 3T measurement setup and vertical device structure with an Al (160 nm)/Mg (1 nm)/Fe (3 nm)/Mg (d_{Mg} nm)/MgO (0.8 nm)/n^+-Si tunnel junction (the thickness of the Mg layer d_{Mg} = 0, 0.5, 1.0, 1.5 and 2.0 nm). It is noteworthy that the MgO layer was not crystallized. To characterize the formation of the dead layer by saturation

magnetization (M_S) measurement, we prepared other samples with the same layered structure and confirmed that a 0.3 nm-thick magnetically-dead layer is formed when d_{Mg} = 0 nm, and that its formation is almost completely prevented when $d_{Mg} \geq 1.0$ nm.
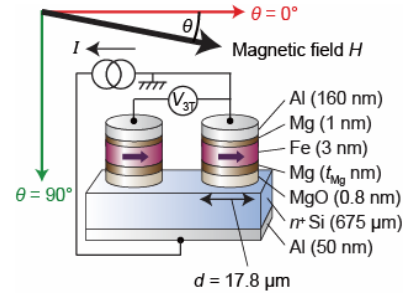

Figure 1 Vertical device structure fabricated on a Si bulk substrate and 3TH measurement setup. Constant current is applied from the backside to the junction (spin extraction regime), and magnetic field applied both in-plane ($\theta = 0°$) and normal to plane ($\theta = 90°$).
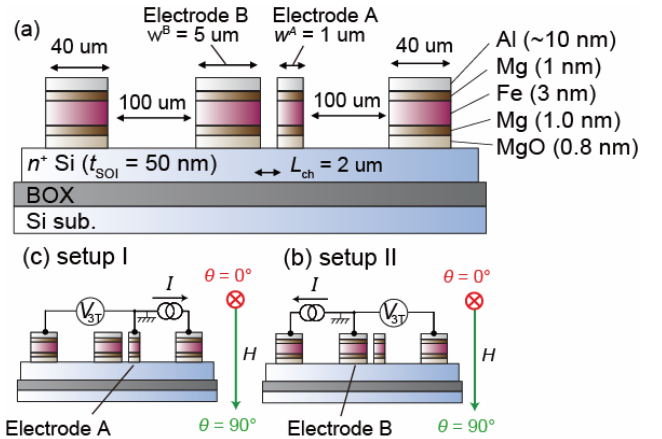

Figure 2 (a) Lateral device structure prepared on a Si-on-insulator (SOI) substrate. (b)(c) 3T measurement setups for electrode A and B.   4T measurement setup is also shown (data is not shown in this abstract).

Figure 2(a) is a lateral device prepared on a (001)-oriented silicon-on-insulator (SOI) substrate, in which the doping concentration of phosphorus and the thickness d_{SOI} of the Si channel layer are ~ 10^{20} cm^{-3} and 50 nm, respectively, the width of electrode A and B are w^A= 1 μm and w^B = 5 μm, respectively. The junction structure is the same as that of the vertical device with d_{Mg} = 1.0 nm.

Figures 2(b) and (c) show 3T measurement setups; 3TH signal of electrode A and B is observed in setup I and II, respectively.

3. Mg thickness dependence of 3TH signals

Figs. 3(a) and (b) show Hanle signals measured with in-plane (red, curve, $\theta = 0°$) and out-of-plane (green curve, $\theta = 90°$) magnetic field, and each black curve is fitting for each signal. Whereas B-3TH is fitted by the multi-angle function derived from the dead layer model [4], and N-3TH signals (Fig. 3(c)) are fitted by following function [5];

$$\Delta V(H) = V_0^{spin} \, \text{Re}\left[\frac{1}{\sqrt{1 + i\gamma\tau_S H}} \right], \qquad (1)$$

where $V_0^{spin} = P^2 J\rho\lambda_S$, P is the spin polarization of the junction, τ_S and λ_S is the spin lifetime and diffusion length in the Si channel, respectively, $\rho = 1$ mΩcm is resistivity of the Si channel, J is the current density, and γ is the gyromagnetic ratio. Consequently, $\tau_S = 1.7$ ns and $P = 16\%$ were estimated, as shown in Fig. 3(c). We found that the magnitude of the B-3TH signal with $\theta = 0°$ decreased with increasing d_{Mg}, and that the N-3TH signal appeared in the samples with $d_{Mg} \geq 1.0$ nm. A notable feature is that the N-3TH increases as the B-3TH (red curve) decreases. All the features of the experimental results agree well with our theory reported in the previous paper [4].

4. 3TH signals variations in different device geometry

Figures 4(a) and (b) show 3TH signals of the lateral device measured in setup I and II, respectively, where red and green curves are the signals measured with in-plane ($\theta = 0°$) and out-of-plane ($\theta = 90°$) magnetic field, respectively. Although the amplitude of the B-3TH signal in the lateral device is almost the same as that in the vertical device, the N-3TH signal became larger than that in the vertical device. Figure 4(c) shows normalized N-3TH signals extracted from Fig.3(c), Figs. 4(a) and (b). The N-3TH signal measured in the lateral device is larger than that in the vertical device, and the signal in setup II is larger than that in setup I. These results are caused by the channel confinement effect, which is prominent in a thin channel and a large electrode. Taking the channel confinement effect into consideration, we originally derived the following fitting function for N-3TH in the lateral device [5]:

$$\Delta V(H) = V_0^{spin} \, \frac{\lambda_S}{t_{SOI}} \, \text{Re}\left[\frac{1}{1 + i\gamma H\tau_S} \left(1 - \frac{1 - e^{-\alpha w}}{\alpha w} \right) \right] (2)$$

where $\alpha = \sqrt{1 + i\gamma H\tau_S} / \lambda_S$ and $w = w^A$ or w^B. The fitting curves are plotted as black curves in Fig. 4(c), in which $\tau_S = 1.3$–1.7 ns and $P = 6.6$–12% were estimated. Since the comparable values of τ_S and P and were obtained in the vertical and lateral devices, the channel confinement should be taken into account for analyzing the spin signals in lateral devices with a thin channel. Note that the spin transport via the Si channel was confirmed by nonlocal 4T Hanle signals in both measurement setups (not shown).
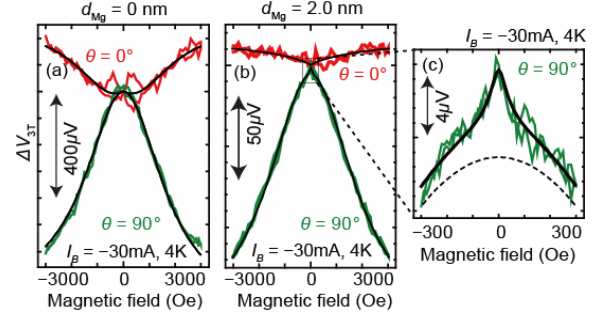

Figure 3　3TH signals obtained in the vertical device with (a) $d_{Mg} = 0$ and (b) $d_{Mg} = 2$ nm. (c) Close up view of the 3TH signal in (b) with $\theta = 90°$.
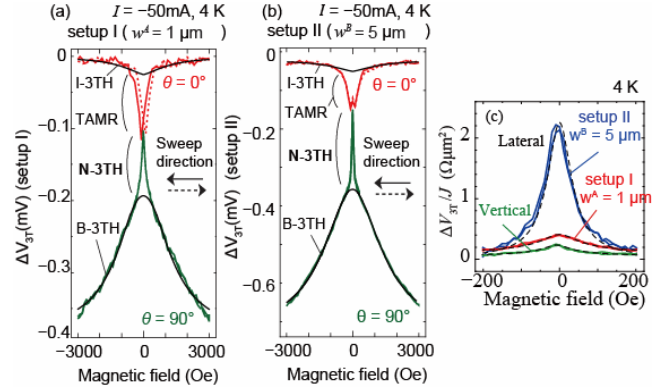

Figure 4　3TH signals obtained in the lateral device with (a) setup I and (b) setup II.　(c) Comparison of the N-3TH signals observed in setup I (red) and II (blue) in the lateral device and in the vertical device (green). The amplitude is normalized by the current density.

5. Conclusions

We have investigated the 3TH signals with the Fe/Mg/MgO/Si junction structures. In the vertical devices, the strong correlation among the B-3TH signals, N-3TH signals, and M_S was clarified when d_{Mg} was varied from 0 to 2 nm. All these experimental features agree well with our theory [4] which predicts that the formation of a dead layer must be prevented for efficient spin injection/detection. In the lateral device, we showed that the N-3TH signals were enhanced by the channel confinement effect, although B-3TH signals were not. We analyzed the N-3TH signals using the function we derived taking into account the device geometry, and obtained the consistent τ_S and P values in both the vertical and lateral devices. As demonstrated in this study, the channel confinement effect should be taken into account for the accurate analysis of spin signals in practical spintronic devices. Our findings will contribute to the unified understanding of spin-dependent transport studies.

References
[1] R. Jansen *et al.*, Semicon. Sci .& Technol. **27**, 083001 (2012).
[2] Y. Aoki et al., PRB **86**, 081201 (2012). [3] O. Txoperena and F. Casanova, J. Phys. D **49**, 133001 (2016). [4] S. Sato et al., APL **107**, 032407 (2015). [5] S. Sato et al., PRB **96**, 235204 (2017).